Ninth Canadian Conference on
Earthquake Engineering
Ottawa, Ontario, Canada
26-29 June 2007

A MECHANICAL MODEL FOR A SUSTAINABLE BUILDING STRUCTURAL SYSTEM

M. Iwata[1] and M. Hirata[2]

ABSTRACT

The authors have developed a sustainable building structure system with a primary goal of extending the service life of the entire structure system and a secondary goal of permitting the reuse of structural members if the primary goal cannot be attained. In this paper, a mechanical model is established, based on the mechanical characteristics of the beam-to-column connection revealed by the authors' past experimental studies. The mechanical model is compared with the results obtained from beam-to-column connection testing. The model is further compared with the results of partial frame testing in which buckling-restrained braces are attached to beams and columns like knee braces. The findings obtained from the comparisons indicate that the mechanical model has satisfactory stiffness and strength, and that it accurately demonstrates the behavior of the beam-to-column connection. Thus, the effectiveness of the model has been proven. The authors believe that the mechanical model is applicable to analysis of the entire structure system.

Introduction

As an architectural effort to reduce the global environmental burden, the authors set a primary goal of extending the service life of the entire structure system. As a secondary goal, they proposed a sustainable building structure system (Fig.1) that permits easy demolition and the reuse of structural members in case the primary goal cannot be attained (Aizawa et al. 2004). By clearly separating the main frame from seismic energy absorption members, this specific structure system serves as a damage-controlled structure that keeps the main frame within the elastic range even when exposed to large earthquakes. The seismic force can be absorbed by buckling-restrained braces alone, braces which are intended to function as seismic-response controlled members. The sustainability of the entire structure system is achieved by replacing only earthquake damaged braces where necessary.

In this study, a mechanical model is developed based on the mechanical characteristics of the beam-to-column connection revealed by the past studies (Okada et al. 2005). Beam-to-column connection testing is performed, and the testing results are compared to the mechanical model to verify its reproducibility. Further, partial frame testing is performed in which buckling-restrained braces are installed as a knee brace, and testing results are compared to the mechanical model to identify its availability when incorporated in the sustainable building structure system.

[1]Professor, Dept. of Architecture and Building Engineering, Kanagawa University, Yokohama, Japan
[2]Graduate Student, Dept. of Architecture and Building Engineering, Kanagawa University, Yokohama, Japan

Beam-to-Column Connection

Fig. 2 illustrates an overview of the beam-to-column connection. A block-shaped joint unit is welded to the beam end. Steel bars with threaded ends are tightened by applying initial tension, thereby connecting the joint unit with the column.

The relationship between the bending moment and the rotational angle at the beam-to-column connection is plotted and presented in Fig.3. As the Figure shows, this relationship is a tri-linear slip model, which can be roughly divided into three stages. The first stage represents the state of the beam-to-column connection from the point where the bending moment acts on the connection to release the initial tension introduced in the steel bars up to the point where the connection is about to separate. When the second stage is reached, the beam-to-column connection is separated and all the steel bars plasticize. The stiffness of the connection declines as compared to the first stage, rendering itself a semi-rigid connection. The third stage represents the state of beam-to-column connection beyond the point where all the steel bars plasticize.

Here, the moments that act on the beam-to-column connection are defined as follows: The bending moment when the beam-to-column connection begins to separate is separate moment M_s, the bending moment when the steel bars begin to plasticize is yield moment M_y, and the bending moment when all the steel bars plasticize is semi-rigid limit moment M_{sem}. Up to the point where M_s is reached, the load increases and decreases along line number one in Fig.3. From the point where the load first goes beyond M_s up to the point where M_{sem} is reached, the load increases along lines two and three, and decreases according to the stiffness indicated by line four. From the second time on, the load increases along line four. Deformation develops along line three. When the load first goes beyond M_{sem}, the stiffness levels off, as indicated by line five, and deformation progresses. The load decreases according to the stiffness indicated by line six. From this point on, the load increases along lines seven, eight, and nine. As described above, stiffness changes step-by-step according to the bending moment that occurs in the beam-to-column connection, thereby both the stiffness requirements of the structural system in use and the deformation capacity requirements when the system is exposed to large earthquakes can be simultaneously fulfilled.

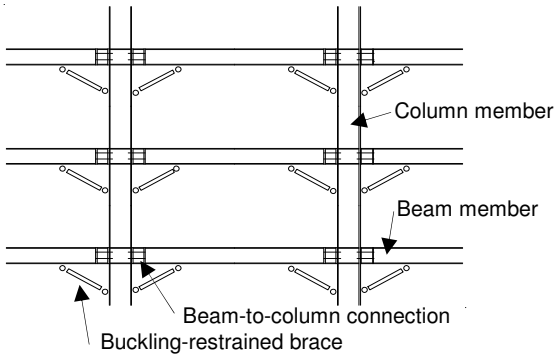

Figure 1. Sustainable building structure system.

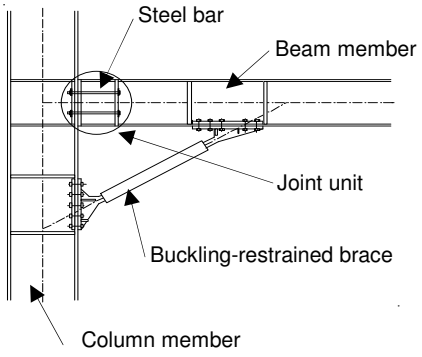

Figure 2. Beam-to-column connection.

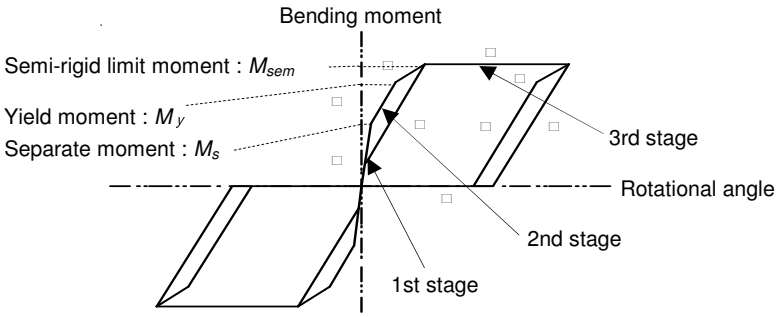

Figure 3. Bending moment – rotational angle relationship.

Beam-to-Column Connection Mechanical Model

In setting a whole structural model of the sustainable building structure, the beam member is divided into Members 1 and 2 (Fig.4-a). Member 1 shown in Fig.4-a is subdivided into three elements of a, b, and c that are connected in a series to each other, as shown in Fig.4-b. Member 2 is a normal line element. Figure 4-c shows Elements a, b, and c in relation to the beam member shown in Fig.2. Element a corresponds to the joint unit in Fig.2. Element c corresponds to the points where the lines connecting the beam cores cross those connecting the brace cores.

The steel bars and flanges consist of modeled axial springs. The parallel and thread parts of the steel bars use axial springs, and these parts are connected in series. As shown in Fig.4-b, l_1 indicates the length of the parallel part, and l_2+l_3, the length of the thread part. Z_1, the length of Element a, is the length between the anchor plate at the upper section of the joint unit and the column flange strengthening plate. Z_2 is the length of Element c, and L is the internal length of Member 1. Based on the hysteretic characteristics modeled in the past studies (Okada et al. 2005), buckling-type hysteretic characteristics are given to the parallel part of the steel bar and slip-type hysteretic characteristics to the thread part, as illustrated in Fig.5.

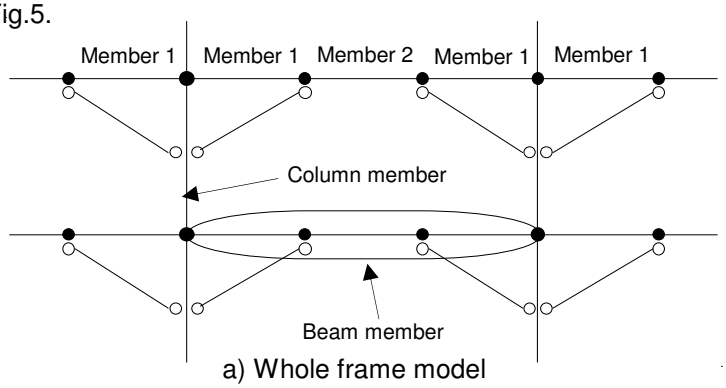

a) Whole frame model

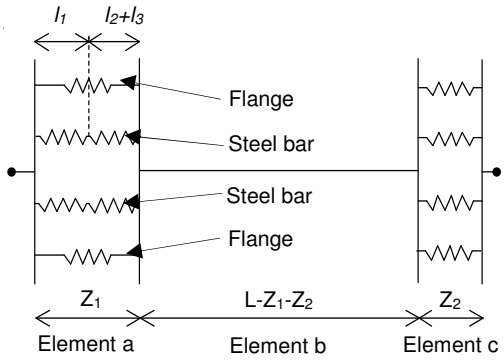

l_1 : Length of the steel bar's parallel part
l_2+l_3 : Length of the steel bar's thread part
Z_1 : Length of Element a
Z_2 : Length of Element c
L : Total Length of Member 1

b) Member 1

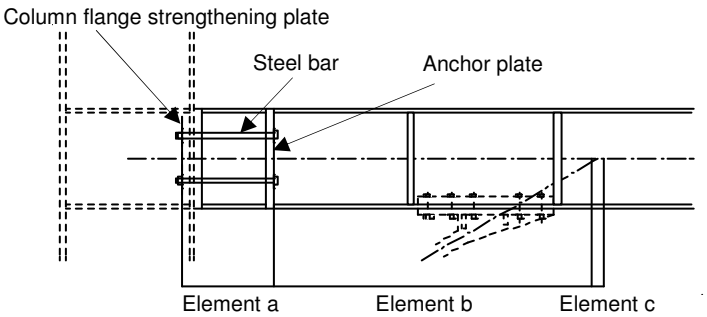

c) Correspondence of beam member and mechanical model

Figure 4. Mechanical model.

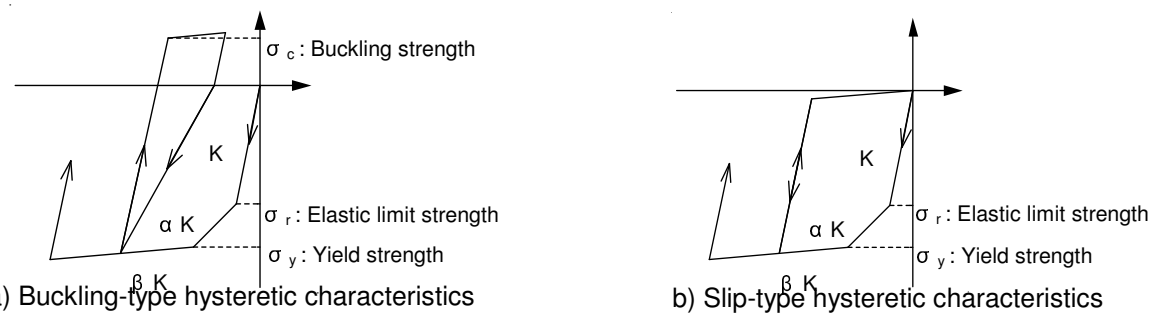

a) Buckling-type hysteretic characteristics b) Slip-type hysteretic characteristics

Figure 5. Hysteretic characteristics of the steel bar.

Comparison with Beam-to-Column Connection Testing

Comparison model overview

Figure 6 shows a comparison model. Figure 6-a illustrates beam-to-column connection testing. Table 1 lists three types of specimens of C1, C2, and C3 used in the test. For all the specimens, four steel bars are placed 75 mm away from the core of the beam member. In analysis, the locations of the steel bars and flanges are converted to the coordinate system presented in Fig.7. In this model, both the x and y coordinates of the steel bars are at the same position as the steel bars of the individual specimens. The x coordinate of the beam member flange is positioned at the center in the flange thickness direction, and the y coordinate, ±75 mm from the beam member core, or the origin of the coordinate.

Using the mechanical model described above, the individual specimens are analyzed. For this purpose, the specimens are converted to the line element model shown in Fig.6-b. Elements a, b, and c shown in this figure correspond to Elements a, b, and c shown in Fig.4-b. In analysis, the Z_1, l_1, and l_2+l_3 of Specimens C1 and C2 are set to 524 mm, 448 mm, and 76 mm, respectively. The Z_1, l_1, and l_2+l_3 of Specimen C3 are set to 324 mm, 248 mm, and 76 mm, respectively. The l_2+l_3 is set to the sum of the lengths of the flange, strengthening plate, and anchor plate of the column member. The steel bar material used in all the specimens is S45C. The yield strength of the individual specimens adopts the tension test results.

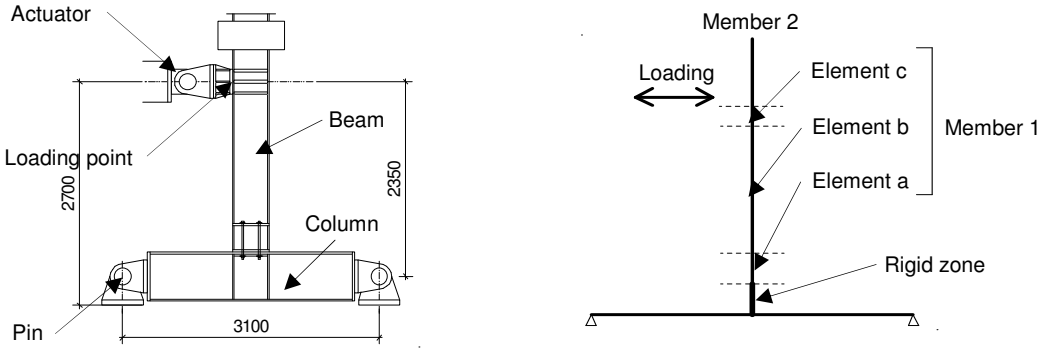

a) Beam-to-column connection b) Line element model

Figure 6. Comparison model

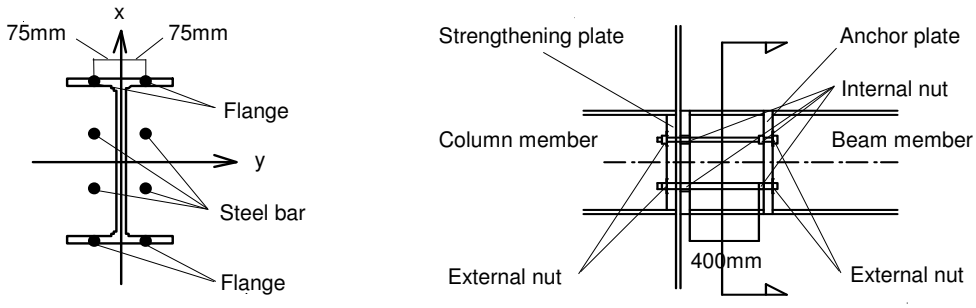

Figure 7. Joint unit cross-section.

Table 1. List of specimens used in the beam-to-column connection test.

Specimen names	Column cross-section	Beam cross-section	Steel bar				
			Material	Young's modulus (N/mm^2)	Yield strength (N/mm^2)	Number of bars (Arrangement)	Length (mm)
C1	H-594×302×14×23	H-440×300×11×18	S45C	2.05×10^5	674	4 (2 rows × 2)	400
C2	H-582×300×12×17	H-300×300×10×15					400
C3	H-482×300×11×15	H-250×250× 9×14					200

In the analytical model setting, in order to compare in detail the correspondence of analytical results with experimental values, the distance between the core of the column and its surface with which the beam comes in contact is set as a rigid zone, as shown in Fig.6-b, and the end of the column member is pin-supported. The stiffness of the web of the joint unit is not considered. In setting the hysteretic characteristics of the steel bar (Fig.5), for both the parallel and thread parts, α is set to 0.25 and β is set to 0.01 for compression, and α and β are set to 0 for tension.

Using these values, the resultant hysteresis loop (full line) obtained from the past study (Okada et al. 2005) is modeled into the dashed line loop presented in Fig.8. In analysis, the loading point is set at 2,350 mm from the column core, as in the test. The value obtained by dividing the horizontal displacement at the loading point by this length is considered to be equivalent to the rotational angle. Alternate cyclic loading is performed in which loads are applied alternately in positive and negative directions, as shown by the loading history presented in Fig.9.

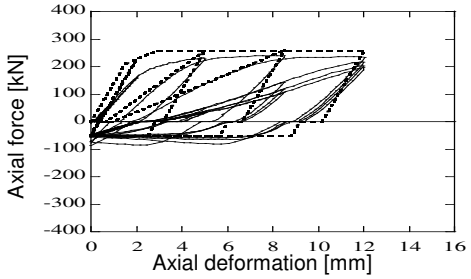

Figure 8. Hysteretic characteristics of the steel bar.

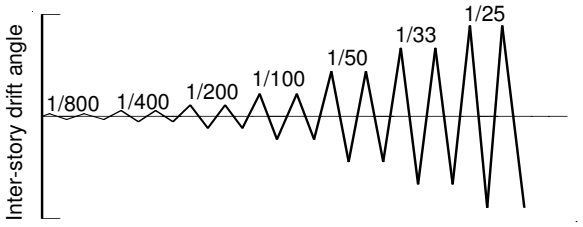

Figure 9. Loading history.

Discussion

The relationships between the bending moment and rotational angle of the individual specimens obtained from the test and analysis are plotted and presented in Fig.10. The full line indicates the test values and the dashed line, the analytical values. In all specimens, the test and analytical values form nearly identical

loops, indicating that the mechanical model accurately represents the relationship between the bending moment and rotational angle.

Figure 11 shows the relationship between the bending moment and rotational angle of Specimen C1 up to the second stage (Fig.3). Both the initial stiffness and separate moment when initial tension is released are accurately expressed by the model. The model is also capable of sufficiently accurate tracking of the changing behavior of the beam-to-column connection after the steel bars yielded. One of the factors that contributes to the error between the test values and the analytical values is that the initial tension could not always be evenly applied to all the steel bars despite the steel bars having been tightened while checking the strain gauges installed at the center of the steel bars.

Figure 12 shows the relationship between the bending moment and rotational angle of Specimen C1 at a rotational angle of 1/25 degrees. The stiffness drop in the first and second hysteresis loops, as well as the slip-type hysteretic characteristics up to the point where the beam flange end comes into contact with the column member, are well represented. The buckling load of the steel bars at a rotational angle of zero degrees is appropriately evaluated, which is the reason for the bending moment not becoming zero.

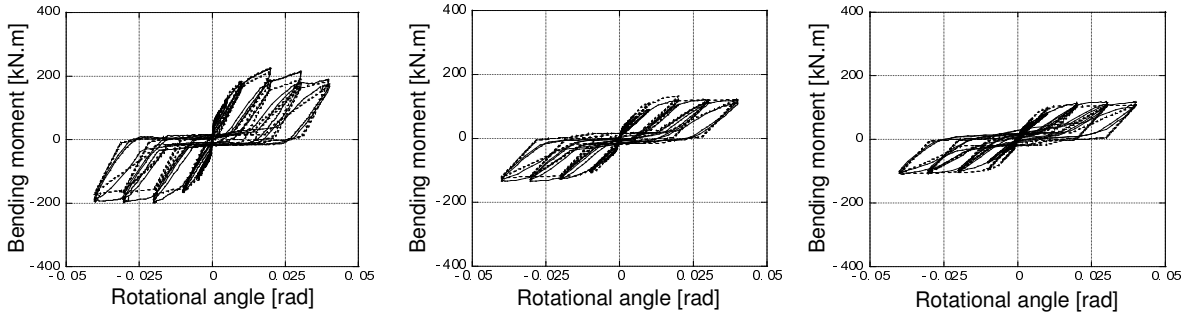

a) Specimen C1 b) Specimen C2 c) Specimen C3

Figure 10. Bending moment – rotational angle relationship.

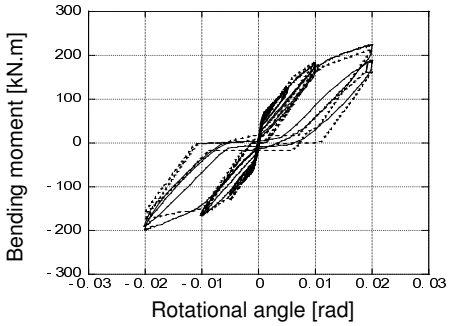

Figure 11. Behavior of the beam-to-column connection in the 2nd stage.

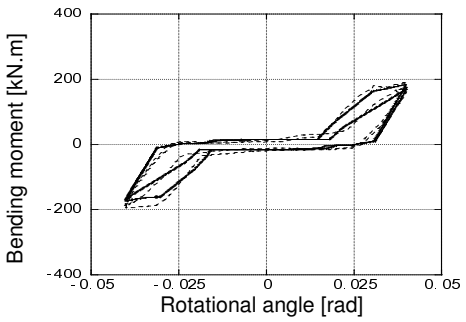

Figure 12. Behavior of the beam-to-column connection at a rotational angle of 1/25 degrees.

Comparison with Partial Frame Testing

The authors intend to reveal the characteristics of the sustainable building structure system in their future studies by tracking the changing behavior of the mechanical model when it is incorporated in the whole frame of the sustainable building structure system. To that end, the effectiveness of the mechanical model when incorporated in a partial frame is confirmed in this study, as this mechanical model is believed to be the smallest possible model to fully grasp the behavior of a partial frame. For this purpose, the results of the alternate cyclic loading test using full-scale specimens that represent partial frames extracted from two-dimensional models are compared with the results of analysis of a partial frame model in which the beam-to-column connection mechanical model is incorporated. Figure 13 shows two-dimensional models,

one with four buckling-restrained braces installed as a knee brace and one with two buckling-restrained braces. These models assume a seven-story (above ground) mid-scale steel-framed apartment building with a story height of 2.75 meters and six 6-meter spans used in the past study (Aizawa et al. 2004). Concerning seismic performance, the first-stage design codes of the Japanese Building Standards Law specify that an inter-story drift angle be less than 1/200 degrees, and that the column and beam members and buckling-restrained braces all be within the elastic range. The second-stage design codes require that an inter-story drift angle be less than 1/100 degrees, and that the beam and column members be within the elastic range, and the buckling-restrained braces be in the plastic range. Based on these conditions, the cross-sectional dimensions of the beam and column members as well as that of the braces' core plates are determined.

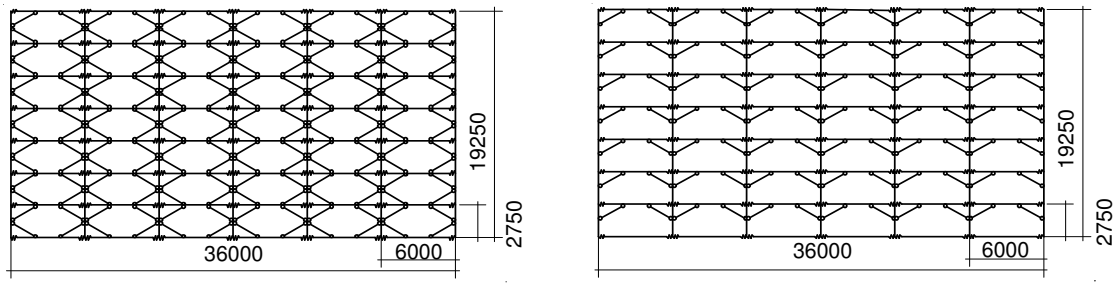

a) 4-brace model b) 2-brace model

Figure 13. Sustainable building structure models.

Table 2. List of specimens used in the partial-frame test.

Specimen names	Column cross-section	Beam cross-section	Steel bar (S45C)	Buckling-restrained brace		
			Yield strength (N/mm^2)	Core plate cross-section	Number of brace	Length of energy absorption part (mm)
F1	H-588×300×12×20	H-300×300×10×15	669.0	PL-80×12	2	1350
F2	H-488×300×11×18	H-294×302×12×12	475.3	PL-80×22		1100
F3	H-588×300×12×20	H-300×300×10×15	478.0	PL-80×22	1	1350
F4	H-588×300×12×20	H-300×300×10×15		PL-80×12		

Comparison model overview

Figure 14 shows a partial frame comparison model. Figures 14-a and 14-c show partial frame testing. Table 2 lists four types of specimens, F1, F2, F3, and F4, which were used in the test. Partial frames are extracted from the mid-level of the 4-brace model (Fig.13-a) and the 2-brace model (Fig.13-b) to serve as Specimens F1 and F3. For Specimen F2, the cross-sectional area of beam and column members is reduced while that of the buckling-restrained brace core plates is increased as compared to Specimen F1. For Specimen F4, beam and column members are designed to have the same cross-sectional area as Specimen F3 while the cross-sectional area of buckling-restrained brace core plates is reduced. In all the specimens, four steel bars are placed 75 mm away from the core of the beam members. In analysis, the locations of the steel bars and flanges are converted to the coordinate system presented in Fig.7, similarly as in beam-to-column connection testing. The steel bar material used is S45C. The yield strength of the individual specimens adopts the tension test results.

Elements a, b, and c in Figs. 14-b and 14-d correspond to Elements a, b, and c in Fig.4-b. In analysis, Z_1 is set to 524 mm, l_1 to 448 mm, and l_2+l_3 to 76 mm for all the specimens.

In the analytical model setting, a rigid zone is set as shown in Figs.14-b and 14-d. The stiffness of the web of the joint unit is not considered. In setting the hysteretic characteristics of the steel bar (Fig.6) for both the parallel and thread parts, α is set to 0.25 and β is set to 0.01 for compression, and α and β are set to 0 for tension. These values are the same as the analytical model setting described above. The buckling-

restrained brace is distinguished between an energy absorption part and a gusset part. The former is a truss member, and the latter, a high-stiffness rectangular member. As shown in Fig.15, the hysteresis loop (full line) obtained from the past study (Kobayashi et al. 2004) is modeled into the dashed-line loop to represent the hysteretic characteristics of the buckling-restrained brace.

The loading point is at 2,350 mm from the column core, as in the test. The value obtained by dividing the horizontal displacement at the loading point by this length is considered to be equivalent to the rotational angle. Alternate cyclic loading is performed in which loads are applied alternately in positive and negative directions, as shown by the loading history presented in Fig.9.

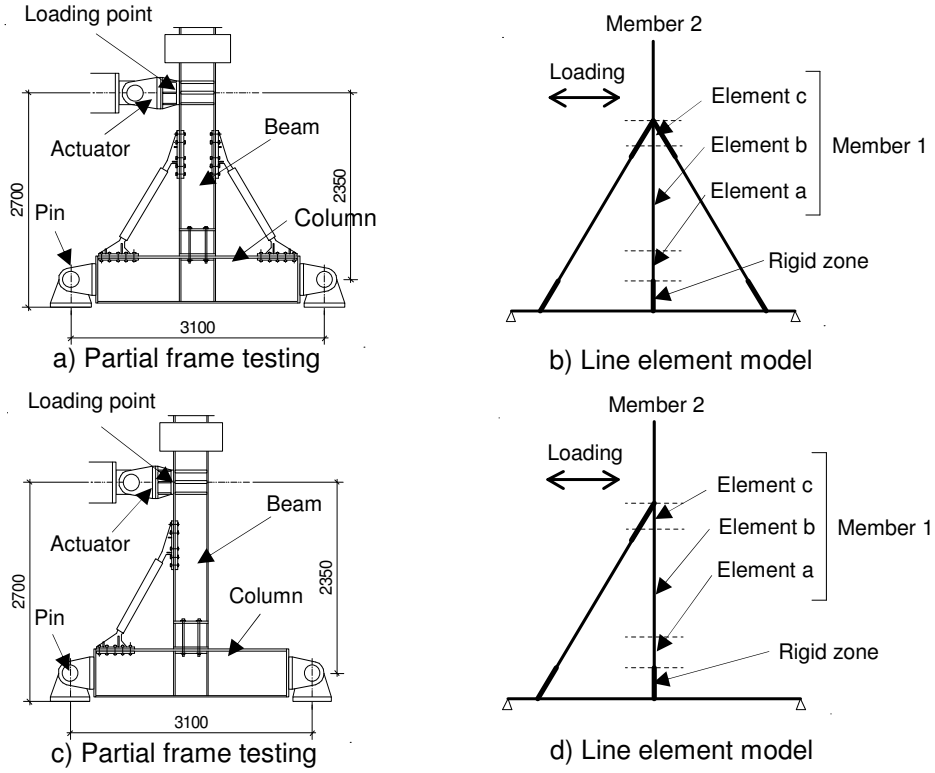

Figure 14. Comparison model.

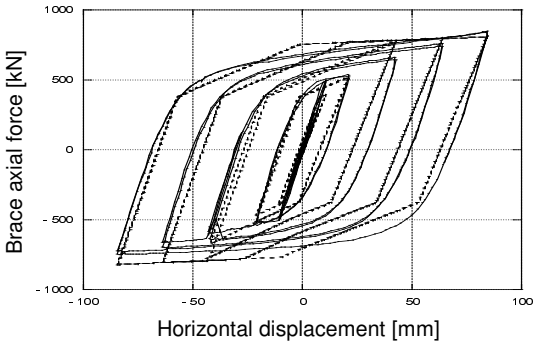

Figure 15. Hysteretic characteristics of the buckling-restrained brace.

Discussion

For the individual specimens, the relationships between load and displacement at the loading point obtained from the test and analysis are plotted and presented in Fig.16. The full line indicates the test

values and the dashed line, the analytical values. In all specimens, both the test and analytical values form nearly identical loops, indicating that the mechanical model accurately represents the relationship between load and displacement at the loading point. When incorporated in the sustainable building structure system, the mechanical model is capable of representing a characteristic feature of the structure system, namely, energy absorption by the buckling-restrained braces after the initial tension of the steel bars was released.

Moreover, the analytical results obtained from Specimens F3 and F4 accurately represent the observed load rise caused by the joint unit end coming into contact with the column flange when load application was switched from compression to tension.

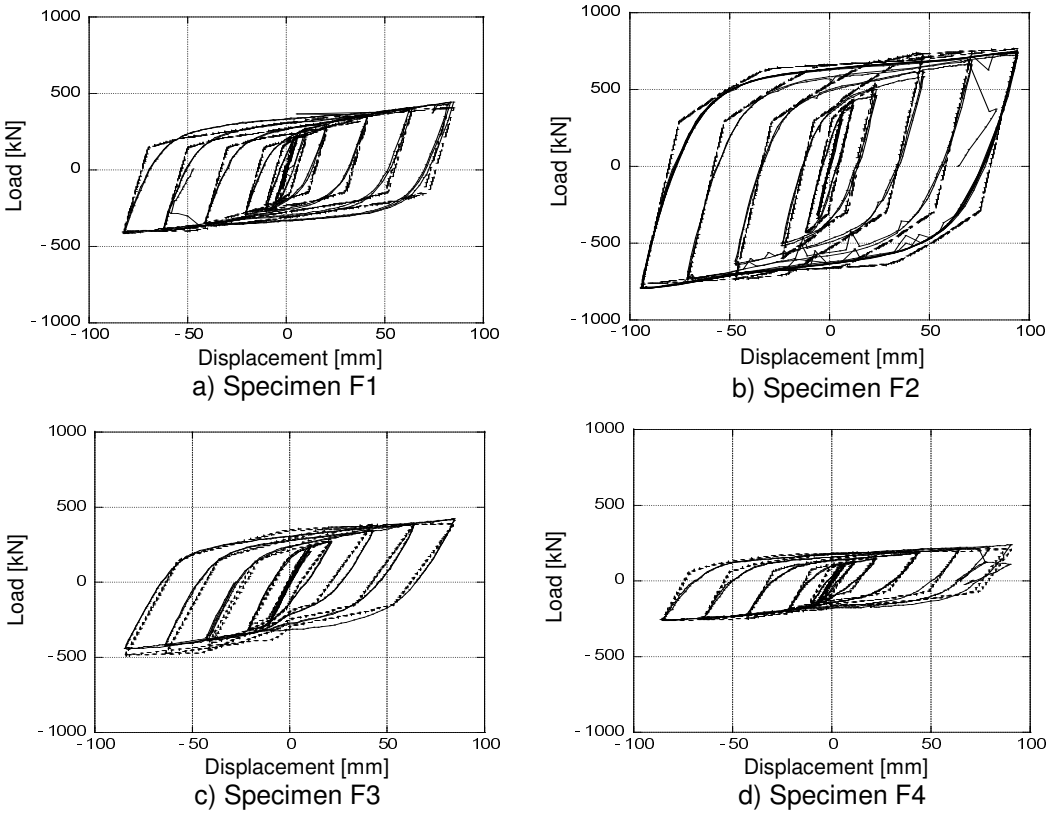

Figure 16. Relationship between load and displacement at the loading point.

Conclusions

In this study, a mechanical model was developed based on the mechanical characteristics of the beam-to-column connection revealed by the past studies. Beam-to-column connection testing was performed, and testing results were compared to this mechanical model. The testing results were further compared to the results of partial frame testing performed using a partial frame with buckling-restrained braces installed as a knee brace. The findings obtained from the above comparisons indicate that the mechanical model is capable of representing the mechanical characteristics of the beam-to-column connection as well as testing results with sufficient accuracy.

This study confirmed that the tracking of the behavior of the mechanical model is possible by incorporating it in the frame of the sustainable building structure system. In future studies, a whole frame model will be designed to identify the characteristics of the sustainable building structure system

Acknowledgments

The authors wish to thank Ms. Mana Nagao, Structure System, Dr. Satoshi Yamada, associate professor at Structural Engineering Research Center, Tokyo Institute of Technology, and Dr. Takeshi Okada, a then researcher at the Center, for their cooperation in performing this study.

References

Aizawa, T., Yamada, S., and Iwata, M., 2004. Proposal of a Sustainable Building Structure and Its Basic Properties, *Journal of environmental engineering (Transaction of AIJ),* No. 581, pp. 109-116.

Okada, T., Yamamoto, S., Yamada, S., and Iwata, M., 2005. Experimental Study on the Beam-to-column Connection in a Sustainable Building Structure System, *Journal of structural and construction engineering (Transaction of AIJ),* No. 591, pp. 145-152.

Kobayashi, F., Murai, M., Izumita, Y, and Iwata, M., 2004. Experimental Study on the Buckling-restrained

Braces Using Steel Mortar Planks (Part II), *Journal of structural and construction engineering (Transaction of AIJ),* No. 586, pp. 187-193.

Iwata, M. and Yamada, S., 2006. Proposal of a Sustainable Building Structure and Its Basic Properties, *STESSA 2006, Behaviour of Steel Structures in Seismic Areas*, pp. 313-319.